

**Jackson State University Mobile Meteorology Data Report**  
**Sundowner Winds Experiment**  
**(SWEX 2022)**

Loren White

Dept of Chemistry, Physics, and Atmospheric Science

Jackson State University

Jackson, MS

Final data submission

September 28, 2024

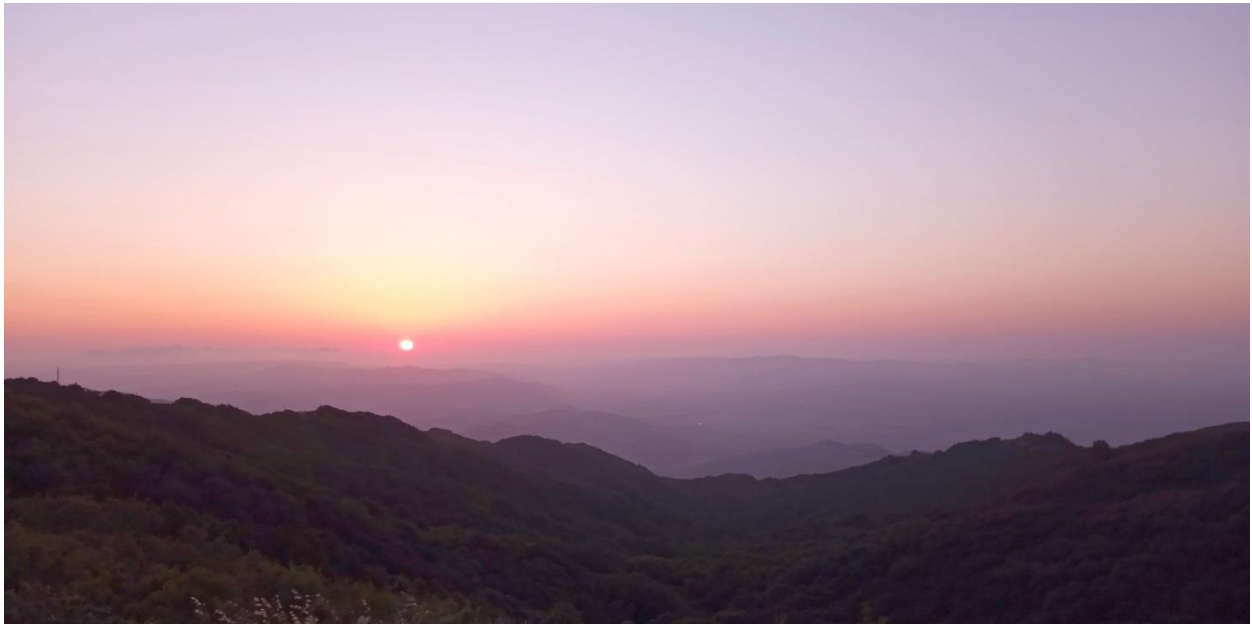


## **Table of Contents**

<b>1 Dataset Overview .....</b>	<b>3</b>
<b>2 Mobile observing system .....</b>	<b>5</b>
<b>3 Data management .....</b>	<b>8</b>
3.1 Quality control .....	8
3.2 Data format .....	12
<b>4 Data summary and metrics .....</b>	<b>13</b>
<b>5 List of IOP/EOP mobile transects .....</b>	<b>14</b>
<b>6 Supplemental mobile and stationary data .....</b>	<b>31</b>
<b>7 References .....</b>	<b>32</b>

## Dataset Overview

The observational campaign of the Sundowner Winds Experiment (SWEX) took place during April 1-May 15, 2022 over a domain near Santa Barbara, California. The goals of SWEX encompass documentation and improved understanding of environmental processes driving the behavior of strong localized winds in the lee of the Santa Ynez Mountains that have often contributed to rapid spread and intensification of wildfires in the region. These winds commonly intensify during the evening hours and are referred to as “sundowner winds”.

To complement various other observational datasets collected for SWEX, mobile measurements were made from instruments mounted on a vehicle operated within the study domain. The mobile platform (JSU Mobile Meteorology Unit—MMU) was based out of Sedgwick Reserve, and generally concentrated on routes determined according to whether a western or eastern mode of sundowner wind forcing was anticipated during the ten IOPs and three EOPs. The main areas of focus can be summarized as:

- *Western Santa Ynez Mountains between Refugio Pass and Santa Ynez Peak*
- *Eastern Santa Ynez Mountains between Brush Peak and Romero Saddle*
- *Mountain gap inland from Gaviota State Park*
- *Coastal margins from Gaviota State Park to Carpinteria*
- *Santa Ynez Valley*

During some transects (mainly along US 101), the JSU MMU followed in tandem behind the UVA WOW mobile lidar. On back-and-forth transect routes (in particular the ridgecrest Camino Cielo segments), typical practice was to wait 30 minutes to one hour when turning around in order to allow conditions to change.

While it was intended to continue collecting mobile data approximately for the same period as the Twin Otter aircraft was overflying the domain, there were a few cases in which MMU operations were terminated early due to mechanical or logistical concerns: IOP 1, IOP 2, IOP 4, EOP 2. In only a few cases was traffic congestion an issue, primarily along US 101 between Santa Barbara and Carpinteria.

Additional mobile data were collected within the SWEX domain by the MMU for various reasons outside of the IOP and EOP days. These are denoted as XOP data, and will be published after the initial data release in hope that they may be relevant to broader understanding of meteorological processes within the area. Similarly, data were collected during the cross-country drive between the JSU MMU home institution inside Mississippi and the Sedgwick Reserve operational base. 4



## Mobile Observing System

A simple platform for mobile observations from a regular **automobile** has been used at JSU since 2012. Currently **temperature** and **humidity** are measured with HC2S (HygroClip) sensors in a 10-plate Gill radiation shield and in an NSSL-style U-tube shield (Waugh 2012), and **solar radiation** by a LiCor pyranometer. Testing by Straka et al. (1996) indicated that, under dry conditions, a Gill-type shield provided superior temperature response at highway speeds compared to the NSSL Mobile Mesonet aspirated system. In heavy rain however, the U-tube (or similar design) is necessary to avoid wet-bulbing effects. Redundant GPS systems with sensitivity up to -185 dB provide position and altitude even under difficult forested conditions. Data are collected once every 2 s on a CR23X datalogger, corresponding to spacing of <60 m even at highway speeds. Derived parameters such as equivalent potential temperature and mixing ratio are calculated in post-analysis. Infrared brightness temperature from an Apogee IRTS is recorded by an upward-looking sensor. The rack for the U-tube is fitted specifically for “Aero” style roof rack crossbars. The vehicle currently being utilized is a 2017 all-wheel drive Subaru Forester (Figure 2).

Wind is not measured by the mobile system. Straka et al. (1996) suggest that wind data with the NSSL Mobile Mesonet were only viable in the absence of nearby obstacles and on straight, flat roads. Neither is practical in forested or mountainous areas. Atmospheric **pressure** is measured by two Vaisala PTB101B barometers within the datalogger enclosure, primarily to facilitate calculation of potential temperature. One barometer is vented to the outside environment through an omnidirectional port. **Photographic** documentation of key route segments is captured by a GoPro Hero 8 camera.

Mobile applications of various configurations of the JSU MMU system have been reported in White (2014), White and Koziara (2018), White (2020), White and Lu (2020), and Butterworth et al. (2021).





*Figure 2: Exterior views of the JSU MMU observing system.*

*Sensors listing:*

CR23X datalogger serial #6182: Recalibrated February 22, 2022

HygroClip serial #20075570: Recalibrated February 22, 2022

HygroClip serial #20075629: Recalibrated February 22, 2022

T109 temperature probe

PTB101B serial #B5020030

PTB101B serial #

LI200 pyranometer

IRTS-P infrared temperature sensor

## **Data Management**

### **Quality Control Procedures**

Following each day of observations, data files were downloaded from the logger to a laptop computer for processing and temporary storage. The primary temperature and humidity measurements were monitored in real time during collection for situational awareness and alert of problems. Following download, initial data checks were made by plotting data as time series, versus distance, and by conversion to a format suitable for spatial viewing in the geographic information system QGIS. Separate transect legs were identified between stops. After spreadsheet calculation of derived and diagnostic quantities, intermediate archival of data files was done on Google Drive. For primary purposes, data collected while stationary for more than a few minutes were removed; however full original data files were retained.

There were no indications in the data of malfunction of the temperature, humidity, radiation, and pressure sensors. Differences in temperature and humidity between redundant sensors were similar to expected based on their different mounting and radiation shielding. Differences between the two barometers were sometimes larger than expected, which may be related to large dynamic pressure effects of gusty winds on the vehicle. There were several instances where problems arose with the primary GPS unit that recorded time, position, and elevation onto the datalogger. In a few cases there were also short data gaps when power supply to the datalogger was interrupted. Data from within the U-Tube shield may have been compromised during IOPs 7 through 9 after power supply to the U-Tube ventilation fan was cut by a severed power cable. It is believed that the cable was struck by debris during strong winds encountered near Gaviota in IOP 7.

### *GPS Errors*

The most critical type of GPS error was loss of accurate position data. In some cases this was apparently due to a reduction in the number of satellites visible to the unit, presumably related to the rugged terrain. In other cases, there was no obvious explanation. Substantial errors or total loss of elevation data (default value of -36) were sometimes, but not always, coincident with position errors. When no valid GPS data were received, the GPS time data were stuck at the last value. Although ground-relative speed is not directly recorded from the GPS data stream, post-processing sometimes revealed an unrealistic oscillation of speed during IOP 9 between subsequent 2-s observing times that was not obvious from plotting the position track. Although occurrence of this oscillation seemed random, it is hypothesized that it is related to a data latency somewhere within communications between the GPS and datalogger.

Very short interruptions of GPS data (for a few seconds) could often be filled directly by linear interpolation (of latitude, longitude, elevation as needed). For longer data gaps, separately archived data from the Garmin Nuvi vehicle navigation system were utilized. Since the Nuvi system routing constrained the position close to its routable road system, it was less prone to errors from satellite availability. As segments of position data were corrected, the newly corrected measurement points, Nuvi data, and data from other transects over the same road were compared at typically about 1:500 scale within QGIS to guard against introduction of errors. An example of position data that were corrected is shown in Figure 3.

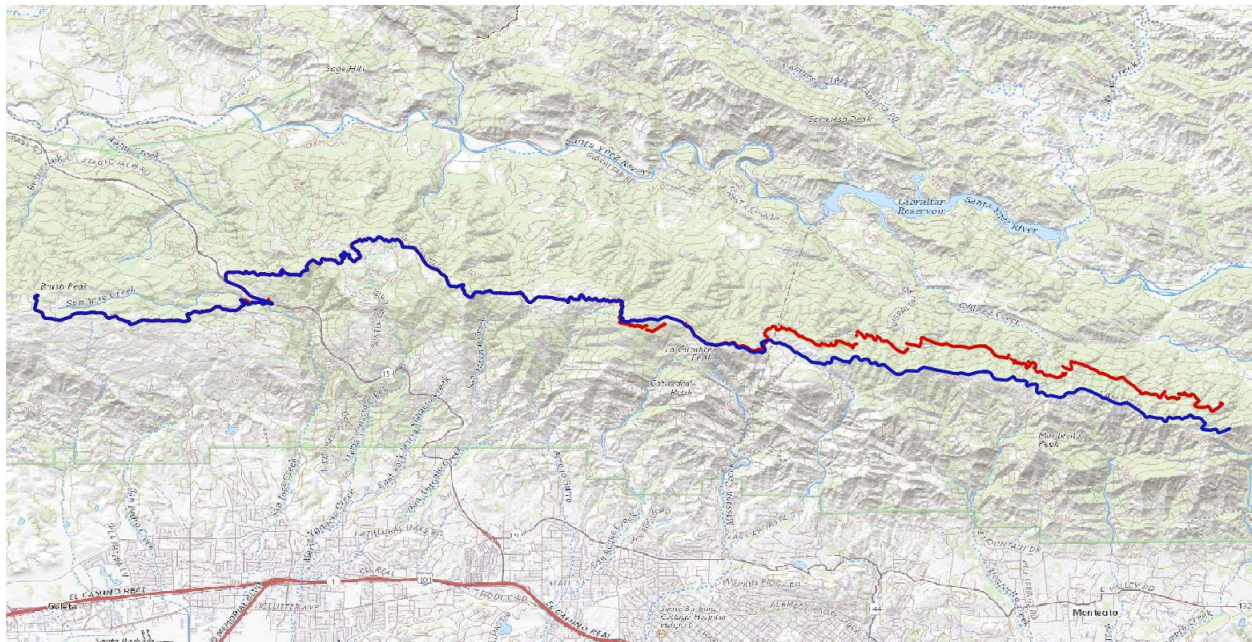


*Figure 3: Comparison of GPS positions during segment 4 of IOP 1 from Brush Peak to Romero Saddle (the worst case of GPS errors). Uncorrected positions are shown in red and corrected positions in blue. The largest displacement was about 700 m.*

One way to identify times when the GPS speed was apparently affected by internal lagging was that the times from the GPS were 1-s behind the time expected to be in step with the 2-s data logging increment. This information was used to interpolate positions to the correct times so that the oscillations were removed. An example of the calculated speeds before and after interpolation is shown in Figure 4.

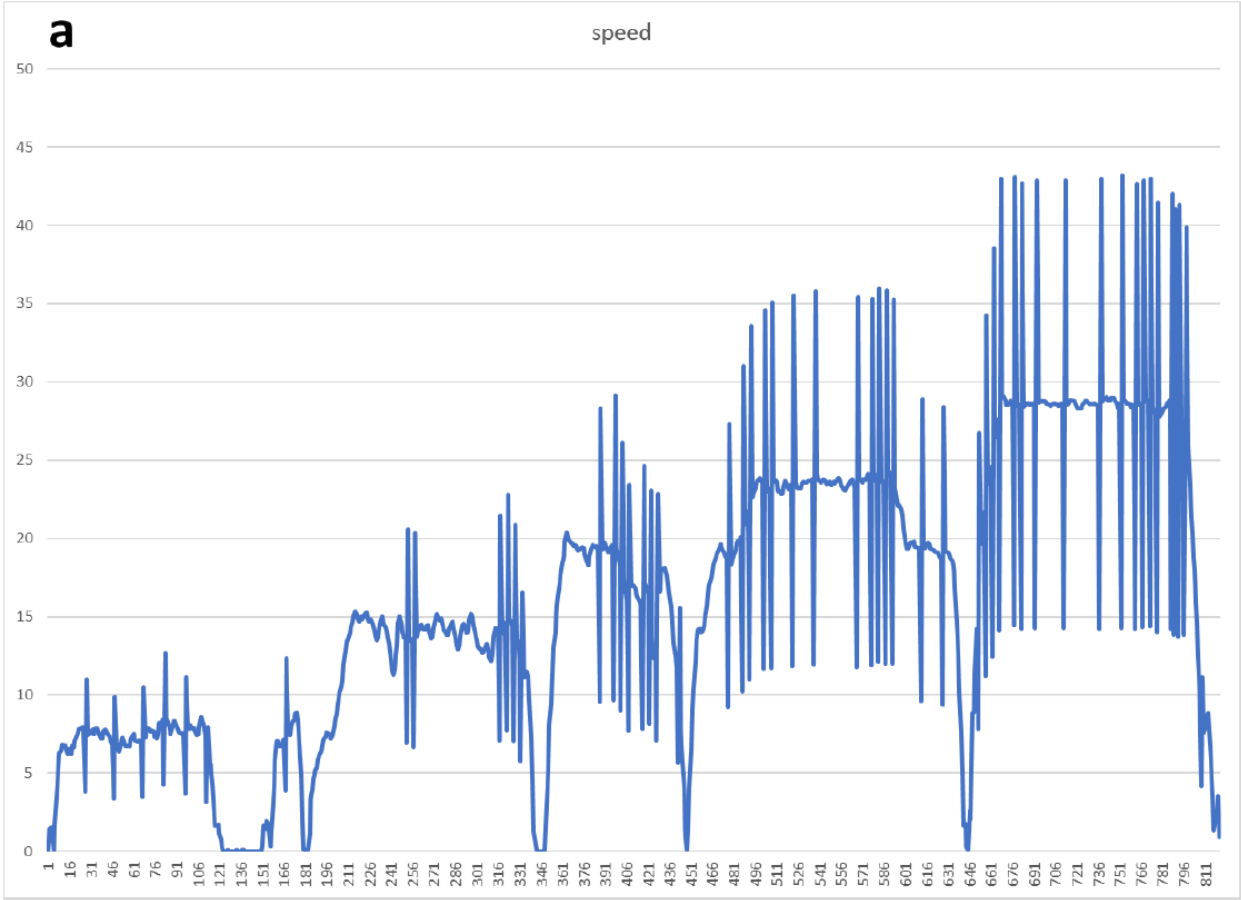




Figure 4: Calculated vehicle speeds from first segment of IOP 9 (Sedgwick Reserve to Buellton) in m/s. (a) Before correction for GPS lag effect; (b) after correction.

GPS time is used as the primary time reference for the dataset. The datalogger times (typically a few seconds off from the GPS) are only used to verify increments when correcting any missing or lagged times from the GPS.

For transects that were affected by GPS issues, an additional data column is added for a flag that indicates times for which GPS data were adjusted (without specifying the type of change).

### Barometers

Based on previous experience, pressure was originally intended to be measured only for use in calculating potential temperature and water vapor mixing ratio. As demonstrated by White (2021), these calculations are fairly insensitive to small differences of pressure (< 5 mb). The few studies of pressure measurements from vehicles have generally preferred use of an omnidirectional external port. However, the current configuration of the JSU MMU uses both a

barometer with an external port and a barometer within the datalogger enclosure within the vehicle. Although efforts were made to calibrate the two barometers before the project, the differences between them during SWEX were often larger than expected. Some of the difference is presumably due to varying response to dynamic pressure effects from air motion relative to the vehicle during motion and variable strong winds. Typical differences are in the range of 1 to 2 mb. An example of pressure differences from a transect with a wide range of vehicle speeds (up to 30 m/s) is shown in Figure 5.

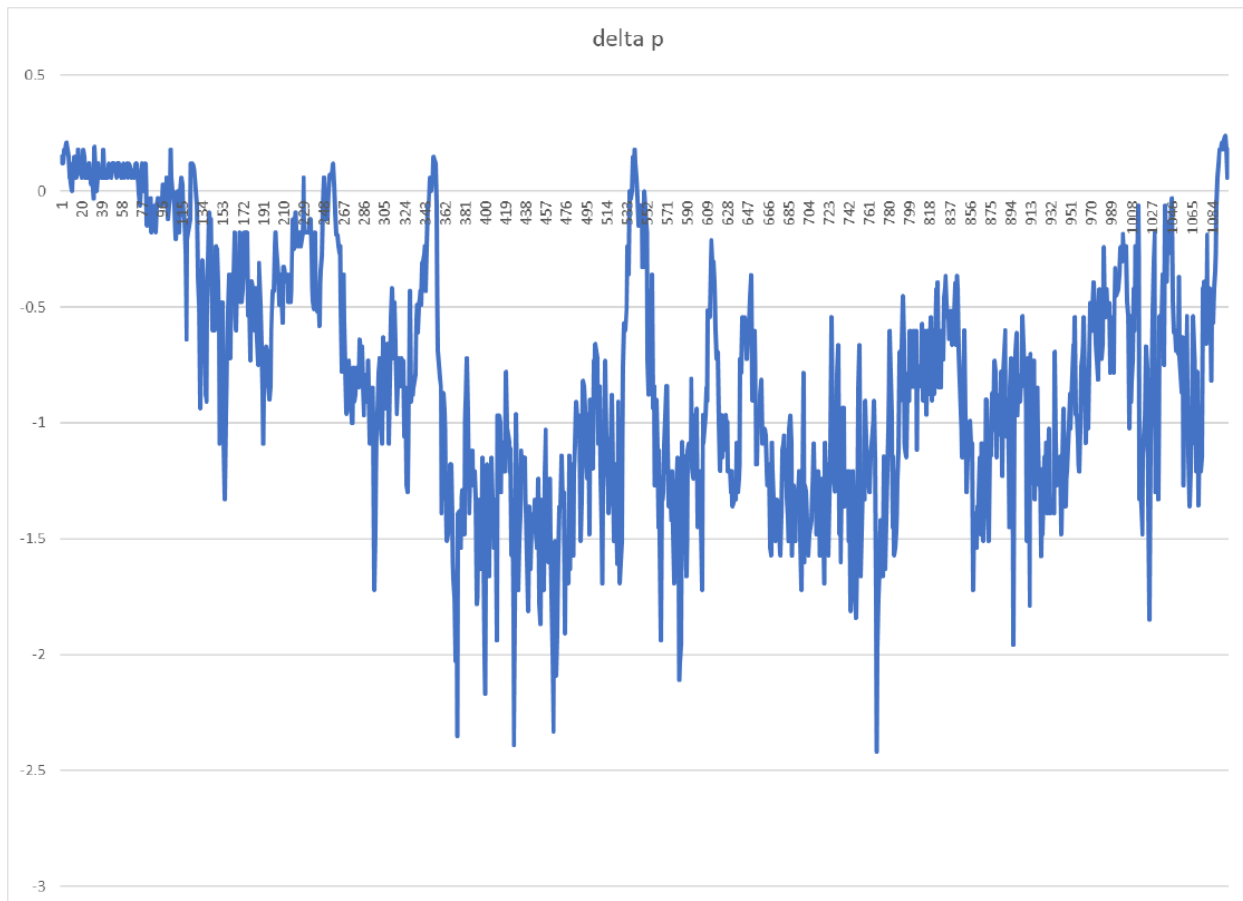


Figure 5: Pressure difference (mb) between barometers during first segment of IOP 6 from Sedgwick Reserve to Mariposa Reina.

### Corrected Elevations

As described in White (2021), true elevation above sea level is not reliably determined by GPS data. In most areas of the United States, accurate gridded elevation data are available with high spatial resolution from the USGS 1/3 arc-second '3DEP' digital elevation model (DEM) dataset. However these elevations do not represent the sensor elevation when the vehicle is on bridges or in tunnels. There is also approximately a 2 m offset between the road surface and the MMU sensors.

To provide an optimal description of the three-dimensional position for measurements, DEM elevations are first interpolated to the MMU track points using the Sample Raster Values tool of QGIS, then a 3-point Gaussian smoother (in time) is applied. We denote the GPS elevation as  $z_g$  and the smoothed DEM elevation as  $\bar{z}$ . Points where data were collected on bridges and in tunnels are determined by plotting the elevations and  $z_g - \bar{z}$ . For each section of roadway that is determined to have DEM elevation differences due to bridges and tunnels, the bordering 'good' DEM points (last, first) are identified. Elevations at these points (where  $\bar{z}$  is affected by neighboring 'bad' points) and all points in between are corrected using slope data from the GPS calibrated to the DEM. The linear approximation of constant slope for these segments was appropriate since all bridges and tunnels driven during the field campaign were monotonic in slope. Points at which elevations are adjusted like this are flagged.

As two extreme examples, the bridge of SR 154 over Cold Spring Canyon goes about 120 m above the bottom of the canyon and the Gaviota Pass tunnel on northbound US 101 is about 60 m below the overlying terrain. While GPS elevation biases away from tunnels and bridges were often only a few meters, in a few cases there were extended periods of biases as large as 100 m.

### **Data Format**

Data from the datalogger are retrieved in native Campbell Scientific .dat format, which is comma-delimited. They are imported into Microsoft Excel to be separated into transect segments and post-processed, including calculation of derived variables, time series plotting, and quality control. Data are then exported to .csv files for spatial plotting in QGIS and archival for EOL.

## Data Summary and Metrics

Temperature and humidity (dewpoint) measurements by sensors within the Gill and U-Tube shields were typically within a few tenths of a degree Celsius. In general, the lower temperatures from the Gill shield are believed to be the most representative due to reduced radiative heating, although the T109 sometimes has an advantage for measurement of rapid changes. The rugged terrain and winding roads were a difficult environment for continuous position determination by GPS. Approximately 3% of observations were affected by GPS issues as noted in the position, elevation, and speed. Corrected positions are believed to be accurate within about 30 m. Comparisons between the two barometers are difficult since they are differently influenced by vehicle air speed.

# of observing points/times (during IOPs/EOPs): 116,966

# of observations with GPS errors: 3356 (2.9% of total)

# of corrected elevations: 1613 (1.4%)

Total distance: 3238.4 km

Maximum speed: 30.8 m/s

Minimum corrected elevation: 0 m

Maximum corrected elevation: 1260 m

Maximum solar/visible radiation: 1640 W/m<sup>2</sup> (presumably influenced by reflection)

Mean Gill shield temperature: 15.7 C

Mean U-Tube temperature: 15.9 C

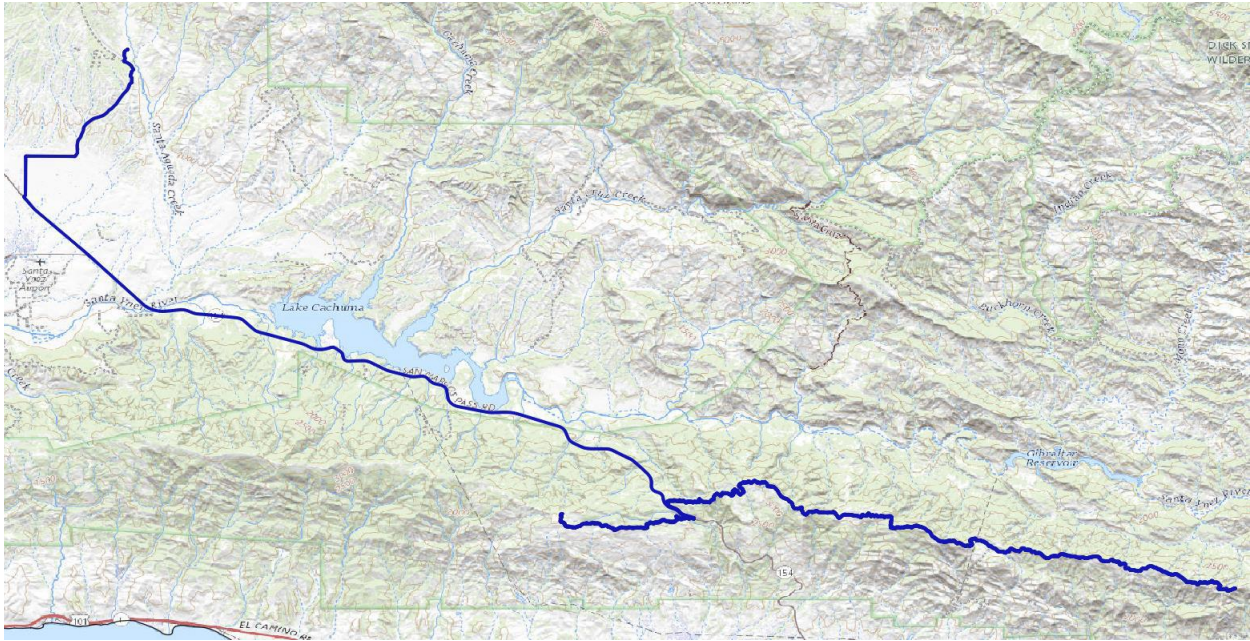
Mean T109 temperature: 15.8 C

Mean Gill shield dewpoint: 3.3 C

Mean U-Tube dewpoint: 3.1 C

## Specifics of IOP/EOP mobile transects

### IOP 1 (April 4-5)



#### Notes:

##### 1. GPS errors

- a. Segment 4: 946 points
- b. Segment 5: 123 points
- c. Segment 6: 5 points

##### 2. Data gap from 04:23:39 to 04:23:59 during segment 7

#### Statistics:

# of obs: 13247

Total distance: 255.0 km

Maximum speed: 25.6 m/s

Minimum corrected elevation: 164 m

Maximum corrected elevation: 1206 m

Maximum solar radiation: 1307 W/m<sup>2</sup>

Mean Gill shield temperature: 18.1 C

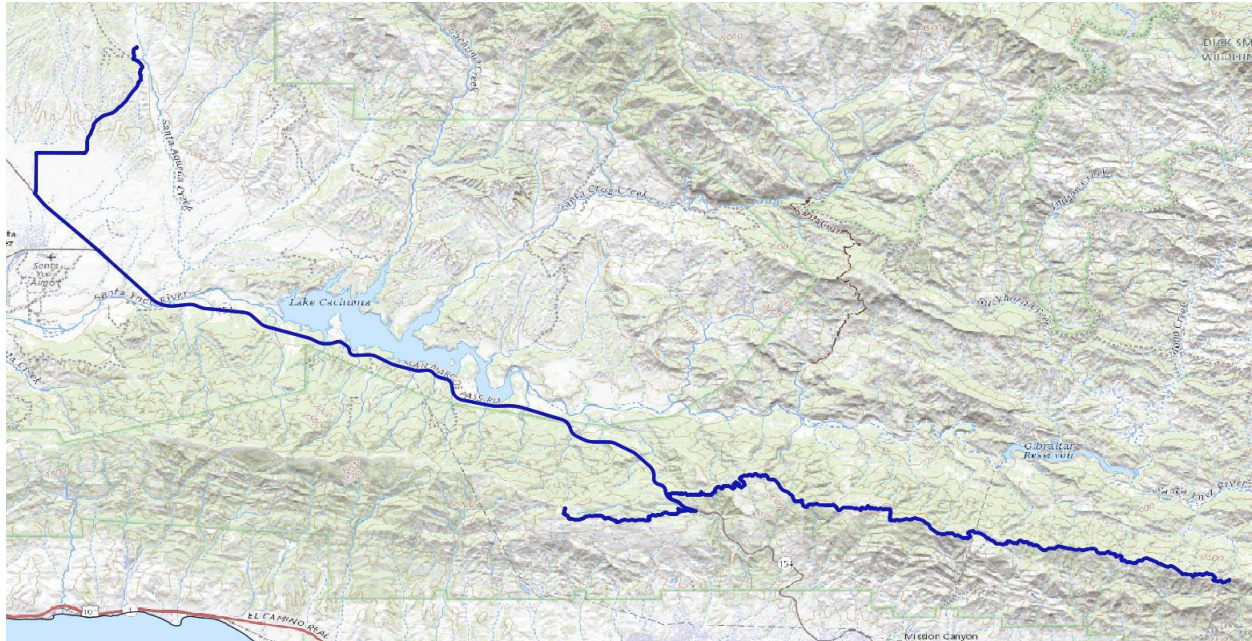
Mean U-Tube temperature: 18.3 C

Mean T109 temperature: 18.2 C

Mean Gill shield dewpoint: 2.4 C

Mean U-Tube dewpoint: 2.2 C

## IOP 2 (April 6)



### Notes:

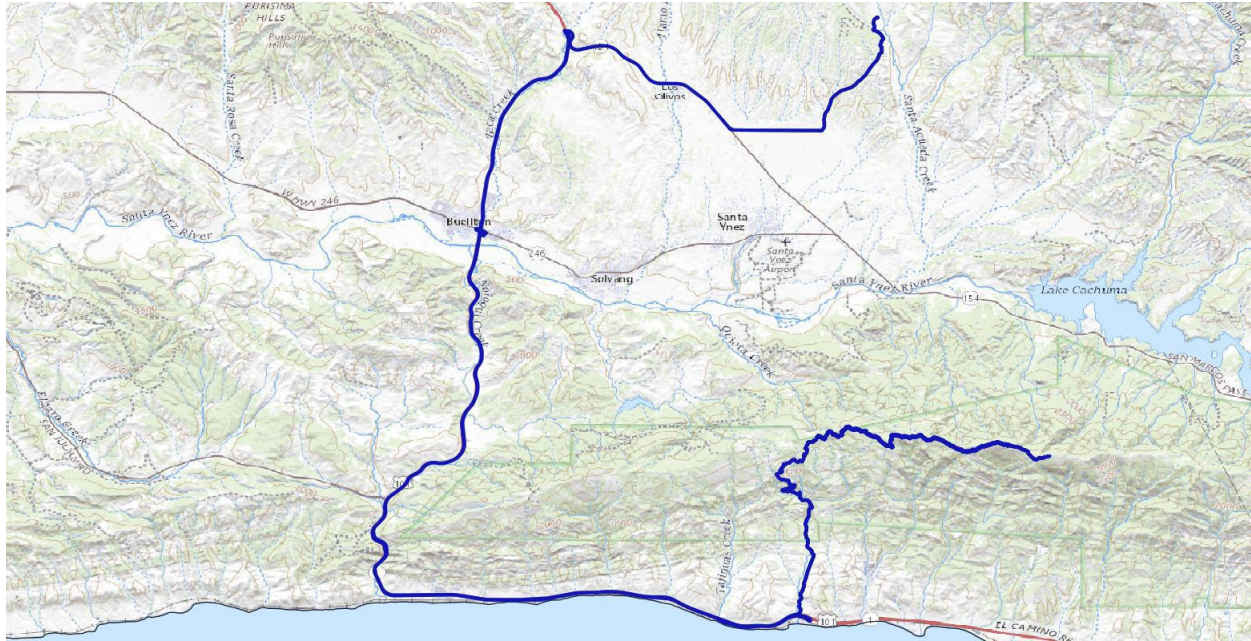
#### 1. Stops within segments

- a. Segment 2: 0223-0226 UTC
- b. Segment 3: 0343-0347 UTC
- c. Segment 4: 0538-0541, 0548-0550 UTC
- d. Segment 5: 0617-0627 UTC

### Statistics:

# of obs: 9027  
Total distance: 176.7 km  
Maximum speed: 25.6 m/s  
Minimum corrected elevation: 165 m  
Maximum corrected elevation: 1206 m  
Maximum solar radiation: 1208 W/m<sup>2</sup>  
Mean Gill shield temperature: 18.1 C  
Mean U-Tube temperature: 18.2 C  
Mean T109 temperature: 18.1 C  
Mean Gill shield dewpoint: 1.0 C  
Mean U-Tube dewpoint: 0.8 C

### IOP 3 (April 13-14)



#### Notes:

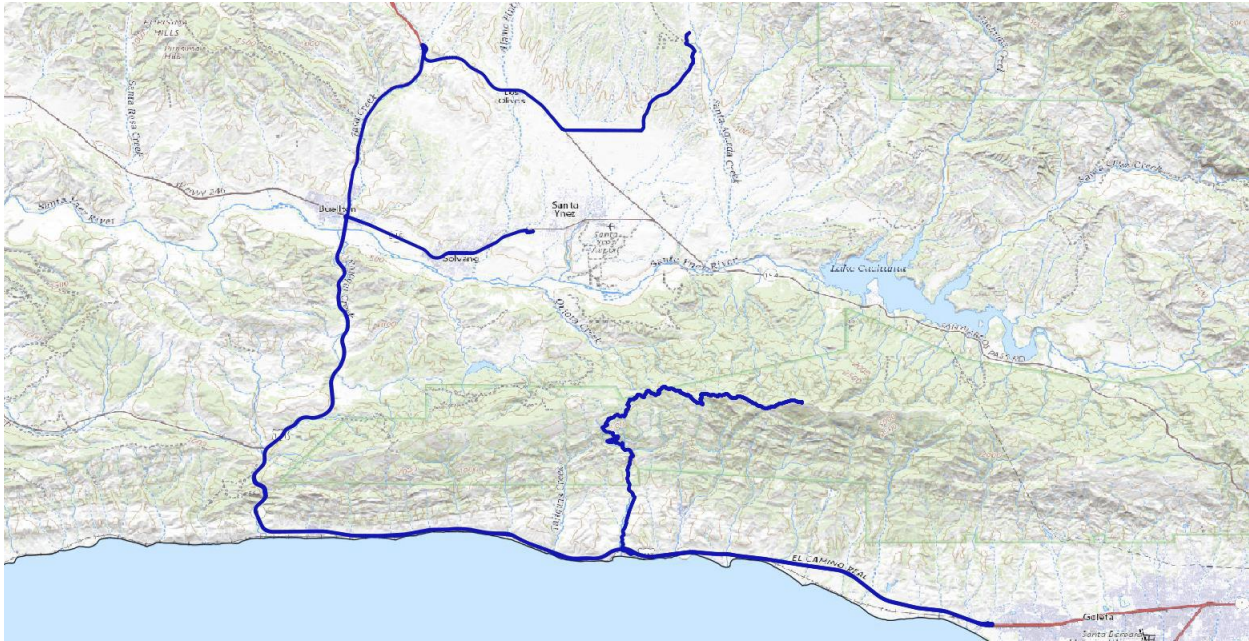
1. GPS errors
  - a. Segment 4: 204 points
  - b. Segment 5: 458 points
2. Stops within segments
  - a. Segment 4: 2040-2043 UTC
  - b. Segment 6: 0103-0105 UTC
  - c. Segment 8: 0315-0324 UTC
  - d. Segment 9: 0400-0402 UTC

#### Statistics:

# of obs: 10871  
Total distance: 209.1 km  
Maximum speed: 29.5 m/s  
Minimum corrected elevation: 11 m  
Maximum corrected elevation: 1254 m  
Maximum solar radiation: 1160 W/m<sup>2</sup>  
Mean Gill shield temperature: 11.7 C  
Mean U-Tube temperature: 11.9 C

Mean T109 temperature: 11.8 C  
Mean Gill shield dewpoint: -0.4 C  
Mean U-Tube dewpoint: -0.6 C

## EOP 1 (April 17-18)



### Notes:

1. Data gap
  - a. Segment 5: 21:32:24 to 21:32:42
2. Stops within segments
  - a. Segment 5: 2135-2137 UTC
  - b. Segment 8: 0047-0048 UTC
  - c. Segment 10: 0239-0243 UTC

### Statistics:

# of obs: 9485  
Total distance: 239.6 km  
Maximum speed: 30.8 m/s  
Minimum corrected elevation: 11 m  
Maximum corrected elevation: 1211 m  
Maximum solar radiation: 1149 W/m<sup>2</sup>  
Mean Gill shield temperature: 14.8 C  
Mean U-Tube temperature: 15.0 C  
Mean T109 temperature: 14.9 C  
Mean Gill shield dewpoint: 8.9 C  
Mean U-Tube dewpoint: 8.7 C

*IOP 4 (April 18-19)*



**Statistics:**

# of obs: 5074

Total distance: 135.3 km

Maximum speed: 29.8 m/s

Minimum corrected elevation: 14 m

Maximum corrected elevation: 1211 m

Maximum solar radiation: 1640 W/m<sup>2</sup>

Mean Gill shield temperature: 17.7 C

Mean U-Tube temperature: 18.0 C

Mean T109 temperature: 17.9 C

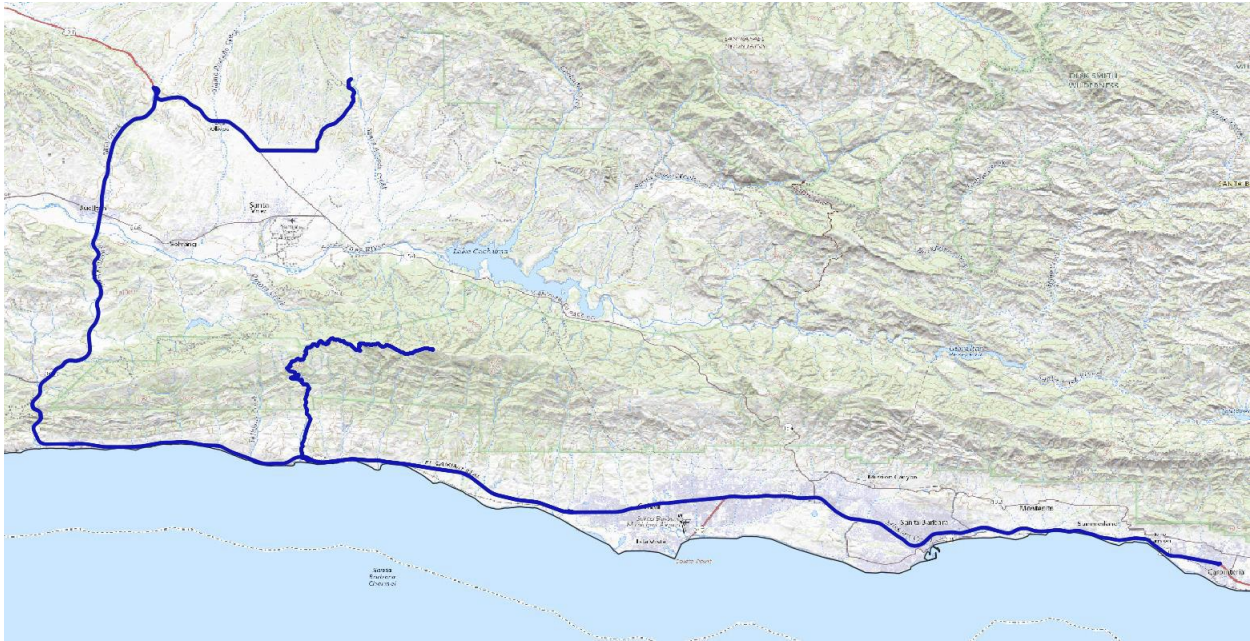
Mean Gill shield dewpoint: 3.9 C

Mean U-Tube dewpoint: 3.6 C





*IOP 6 (April 28-29)*



**Statistics:**

# of obs: 9568

Total distance: 316.1 km

Maximum speed: 29.5 m/s

Minimum corrected elevation: 5 m

Maximum corrected elevation: 1210 m

Maximum solar radiation: 978 W/m<sup>2</sup>

Mean Gill shield temperature: 12.6 C

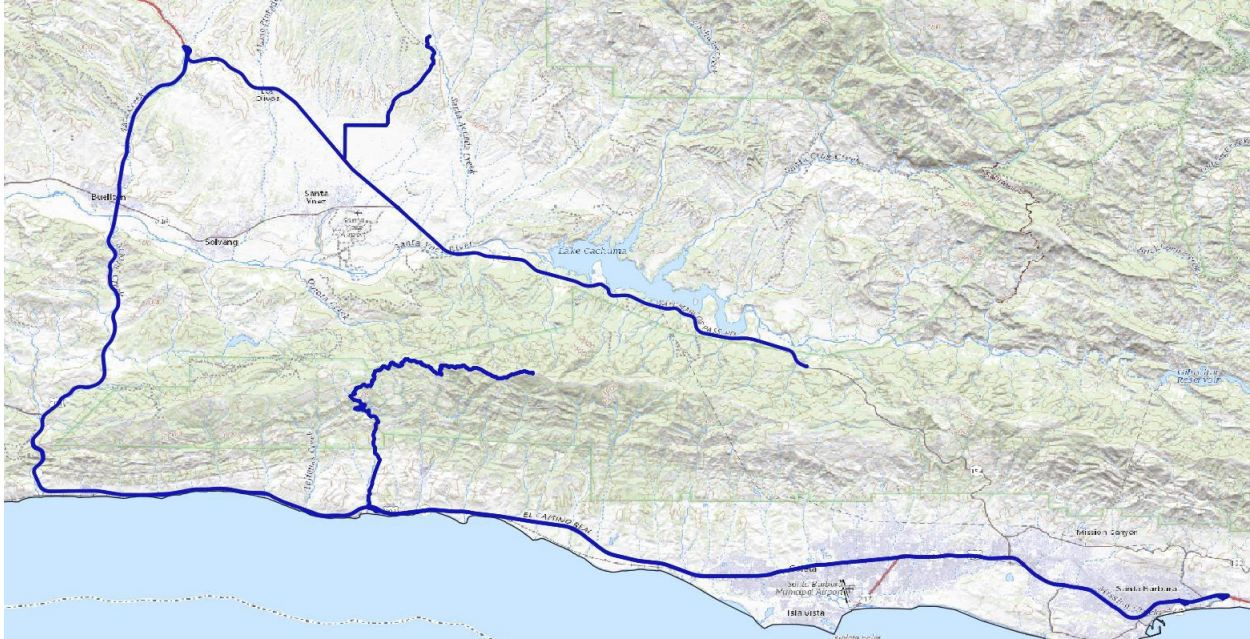
Mean U-Tube temperature: 12.7 C

Mean T109 temperature: 12.6 C

Mean Gill shield dewpoint: 5.4 C

Mean U-Tube dewpoint: 5.2 C

## EOP 3 (May 4-5)



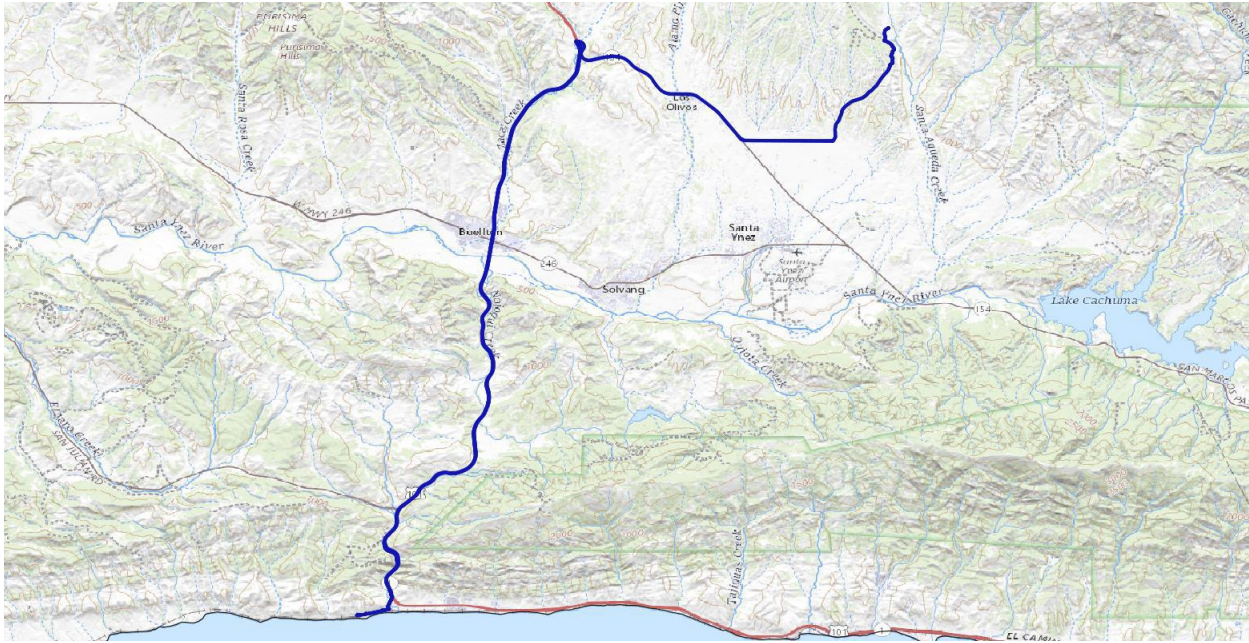
### Notes:

1. GPS errors
  - a. Segment 6: 254 points
  - b. Segment 7: 214 points
  - c. Segment 8: 4 points
  
2. Stops within segments
  - a. Segment 11: 0300-0302 UTC

### Statistics:

# of obs: 12429  
Total distance: 408.2 km  
Maximum speed: 29.6 m/s  
Minimum corrected elevation: 5 m  
Maximum corrected elevation: 1210 m  
Maximum solar radiation: 985 W/m<sup>2</sup>  
Mean Gill shield temperature: 20.0 C  
Mean U-Tube temperature: 20.2 C  
Mean T109 temperature: 20.1 C  
Mean Gill shield dewpoint: 6.0 C  
Mean U-Tube dewpoint: 5.7 C

## IOP 7 (May 7-8)



### Notes:

1. GPS errors
  - a. Segment 6: 14 points

### Statistics:

# of obs: 4987  
Total distance: 204.6 km  
Maximum speed: 30.0 m/s  
Minimum corrected elevation: 6 m  
Maximum corrected elevation: 371 m  
Maximum solar radiation: 899 W/m<sup>2</sup>  
Mean Gill shield temperature: 13.8 C  
Mean U-Tube temperature: 14.0 C  
Mean T109 temperature: 13.8 C  
Mean Gill shield dewpoint: 6.8 C  
Mean U-Tube dewpoint: 6.6 C

## IOP 8 (May 8-9)



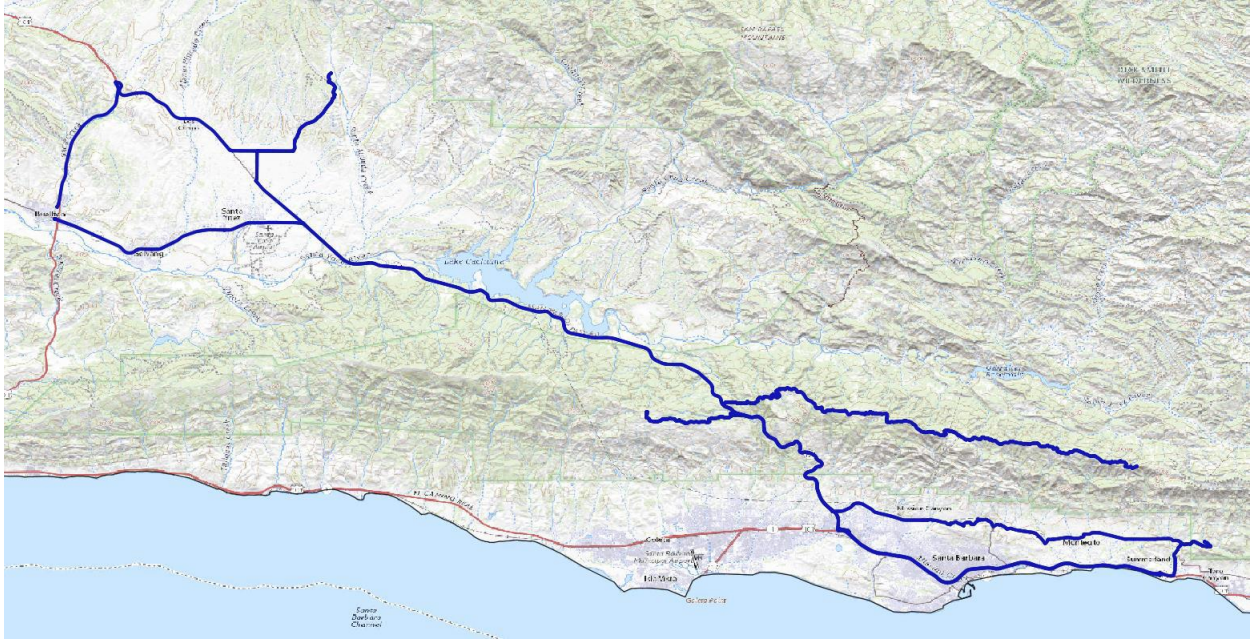
### Notes:

1. Stops within segments
  - a. Segment 5: 0006-0008, 0013-0015 UTC

### Statistics:

# of obs: 9531  
Total distance: 373.6 km  
Maximum speed: 30.1 m/s  
Minimum corrected elevation: 6 m  
Maximum corrected elevation: 692 m  
Maximum solar radiation: 1080 W/m<sup>2</sup>  
Mean Gill shield temperature: 14.7 C  
Mean U-Tube temperature: 14.9 C  
Mean T109 temperature: 14.7 C  
Mean Gill shield dewpoint: 2.5 C  
Mean U-Tube dewpoint: 2.3 C

## IOP 9 (May 10-11)



### Notes:

#### 1. GPS errors

- a. Segment 1: speed errors at 58 points
- b. Segment 2: speed errors at 5 points
- c. Segment 5: speed errors at 500 points
- d. Segment 6: speed errors at 34 points
- e. Segment 7: speed errors at 21 points
- f. Segment 8: speed errors at 516 points

### Statistics:

# of obs: 11958

Total distance: 316.5 km

Maximum speed: 29.3 m/s

Minimum corrected elevation: 6 m

Maximum corrected elevation: 1206 m

Maximum solar radiation: 956 W/m<sup>2</sup>

Mean Gill shield temperature: 10.2 C

Mean U-Tube temperature: 10.3 C

Mean T109 temperature: 10.1 C

Mean Gill shield dewpoint: 0.7 C

Mean U-Tube dewpoint: 0.5 C



Period	Leg	Year	Month	Day	Begin UTC	End UTC	From	To	km	
IOP 1	1	2022	4	4	1843	1931	Sedgwick Reserve	Brush Peak	46.5	
	2				1937	2039	Brush Peak	Romero Saddle	36.0	
	3				2106	2213	Romero Saddle	Brush Peak	36.0	
	4				2340	0048	Brush Peak	Romero Saddle	36.3	
	5				0058	0203	Romero Saddle	Brush Peak	35.9	
	6				0230	0343	Brush Peak	Romero Saddle	36.1	
	7				0404	0459	Romero Saddle	San Marcos Pass	28.2	
IOP 2	1	2022	4	6	0058	0147	Sedgwick Reserve	Brush Peak	46.4	
	2				0201	0313	Brush Peak	Romero Saddle	36.0	
	3				0330	0453	Romero Saddle	Brush Peak	35.9	
	4				0521	0557	Brush Peak	Tower 9	13.4	
	5				0603	0705	Tower 9	Sedgwick Reserve	45.0	
IOP 3	1	2022	4	13	1831	1858	Sedgwick	Buellton, CA	26.7	
	2				1909	1954	Buellton, CA	Refugio Pass	45.1	
	3				2003	2047	Refugio Pass	Santa Ynez Peak	10.7	
	4				2204	2233	Santa Ynez Peak	Refugio Pass	9.8	
	5				2321	2344	Refugio Pass	Tower 8	8.9	
	6				14	0050	0117	Tower 8	Refugio Pass	8.9
	7			0147		0212	Refugio Pass	Tower 8	8.9	
	8			0300		0337	Tower 8	Refugio Pass	8.9	
	9			0346		0418	Refugio Pass	Refugio Beach	11.4	
	10			0421		0431	Refugio Beach	Circle Bar B	5.3	
	11			0432		0441	Circle Bar B	Refugio Beach	5.3	
	12			0442	0533	Refugio Beach	Sedgwick Reserve	59.2		
EOP 1	1	2022	4	17	1955	2016	Solvang, CA	Gaviota SP	25.6	
	2				2021	2040	Gaviota SP	Goleta, CA	31.2	
	3				2046	2056	Goleta, CA	Refugio Beach	15.5	
	4				2056	2119	Refugio Beach	Refugio Pass	11.4	
	5				2125	2150	Refugio Pass	Tower 8	8.9	
	6				2235	2257	Tower 8	Refugio Pass	8.9	
	7				2333	2356	Refugio Pass	Tower 8	9.0	
	8				18	0033	0057	Tower 8	Refugio Pass	8.9
	9					0132	0155	Refugio Pass	Tower 8	8.9
	10					0236	0305	Tower 8	Refugio Pass	8.9
	11					0331	0359	Refugio Pass	Refugio Beach	11.7
	12					0359	0410	Refugio Beach	Goleta, CA	15.6
	13				0410	0429	Goleta, CA	Gaviota SP	30.8	
	14			0429	0506	Gaviota SP	Sedgwick Reserve	44.3		

IOP 4	1	2022	4	18	2010	2035	Sedgwick Reserve	Buellton, CA	25.9	
	2				2057	2111	Buellton, CA	San Onofre Beach	22.3	
	3				2218	2223	San Onofre Beach	Mariposa Reina	4.2	
	4				2232	2252	Mariposa Reina	Goleta, CA	29.0	
	5				2253	2303	Goleta, CA	Refugio Beach	15.8	
	6				2308	2331	Refugio Beach	Refugio Pass	11.3	
	7				2338	0001	Refugio Pass	Tower 8	8.9	
	8				19	0039	0101	Tower 8	Refugio Pass	8.9
	9				0131	0154	Refugio Pass	Tower 8	9.0	
IOP 5	1	2022	4	23	2254	2332	Sedgwick Reserve	Mariposa Reina	46.4	
	2				2337	0022	Mariposa Reina	Carpinteria, CA	67.1	
	3				24	0041	0120	Carpinteria, CA	Brush Peak	42.3
	4				0147	0257	Brush Peak	Romero Saddle	35.9	
	5				0336	0445	Romero Saddle	Brush Peak	35.9	
	6				0453	0534	Brush Peak	Carpinteria, CA	42.3	
	7				0535	0655	Carpinteria, CA	Sedgwick Reserve	113.4	
EOP 2	1	2022	4	25	2154	2219	Sedgwick Reserv	Buellton, CA	26.7	
	2				2225	2238	Buellton, CA	Mariposa Reina	19.6	
	3				2306	2334	Mariposa Reina	Santa Barbara, CA	42.4	
	4				2335	2358	Santa Barbara, CA	Brush Peak	17.9	
	5				26	0111	0223	Brush Peak	Romero Saddle	36.1
IOP 6	1	2022	4	28	2227	2304	Sedgwick Reserve	Mariposa Reina	46.3	
	2				2315	2334	Mariposa Reina	Goleta, CA	28.9	
	3				2335	2345	Goleta, CA	Refugio Beach	15.9	
	4				2355	0018	Refugio Beach	Refugio Pass	11.3	
	5				29	0033	0054	Refugio Pass	Tower 8	8.9
	6				0135	0156	Tower 8	Refugio Pass	8.9	
	7				0232	0255	Refugio Pass	Tower 8	8.9	
	8				0325	0347	Tower 8	Refugio Pass	8.9	
	9				0353	0417	Refugio Pass	Refugio Beach	11.9	
	10				0422	0459	Refugio Beach	Carpenteria, CA	53.0	
	11				0459	0620	Carpenteria, CA	Sedgwick Reserve	113.2	
EOP 3	1	2022	5	4	1911	1943	Sedgwick Reserve	Paradise Rd	34.5	
	2				1947	2013	Paradise Rd	US 101	35.3	
	3				2013	2030	SR 154	Gaviota SP	27.3	
	4				2030	2104	Gaviota SP	Santa Barbara, CA	55.4	
	5				2105	2130	Santa Barbara, CA	Refugio Beach	40.6	
	6				2143	2206	Refugio Beach	Refugio Pass	11.4	
	7				2245	2306	Refugio Pass	Santa Ynez Peak	8.8	
	8				2348	0008	Santa Ynez Peak	Refugio Pass	8.9	

				9		5	0035	0057	Refugio Pass	Santa Ynez Peak	9.0	
				10			0146	0207	Santa Ynez Peak	Refugio Pass	8.9	
				11			0249	0316	Refugio Pass	Santa Ynez Peak	8.9	
				12			0348	0411	Santa Ynez Peak	Refugio Pass	8.9	
				13			0418	0443	Refugio Pass	Refugio Beach	11.3	
				14			0454	0518	Refugio Beach	Santa Barbara, CA	38.9	
				15			0520	0552	Santa Barbara, CA	Gaviota SP	53.2	
				16			0552	0609	Gaviota SP	SR 154	27.2	
				17			0609	0630	US 101	Sedgwick Reserve	19.7	
IOP 7	1	2022				5	7	2242	2319	Sedgwick Reserve	Gaviota SP	44.8
	2						8	0217	0237	Gaviota SP	SR 154	28.0
	3							0237	0259	SR 154	Gaviota SP	28.8
	4							0350	0411	Gaviota SP	SR 154	28.6
	5							0411	0430	SR 154	Gaviota SP	27.8
	6							0444	0522	Gaviota SP	Sedgwick hill	43.8
	7							0522	0531	Sedgwick Reserve	Sedgwick Reserve	2.8
IOP 8	1	2022				5	8	2126	2204	Sedgwick Reserve	Gaviota SP	44.8
	2							2302	2320	Mariposa Reina	Goleta, CA	28.9
	3							2321	2331	Goleta, CA	Refugio Beach	15.9
	4							2332	2356	Refugio Beach	Refugio Pass	11.3
	5						9	0000	0029	Refugio Pass	Refugio Beach	11.2
	6							0038	0058	Refugio Beach	Santa Barbara, CA	29.6
	7							0059	0114	Santa Barbara, CA	Paradise Rd	17.3
	8							0114	0141	Paradise Rd	US 101	35.2
	9							0141	0200	SR 154	Gaviota SP	27.9
	10							0212	0233	Gaviota SP	SR 154	28.0
	11							0233	0251	SR 154	Mariposa Reina	29.2
	12							0337	0406	Mariposa Reina	Santa Barbara, CA	42.7
	13							0407	0422	Santa Barbara, CA	Paradise Rd	17.2
	14							0422	0455	Paradise Rd	Sedgwick Reserve	34.4
IOP 9	1	2022				5	10	2024	2251	Sedgwick Reserve	Buellton, CA	25.8
	2							2304	2348	Buellton, CA	SR 192 (Foothill Rd)	50.9
	3							2349	0022	SR 154	Toro Canyon Park	21.9
	4						11	0114	0158	Toro Canyon Park	Brush Peak	40.4
	5							0216	0337	Brush Peak	Romero Saddle	36.0
	6							0417	0529	Romero Saddle	Brush Peak	36.1
	7							0538	0614	Brush Peak	Summerland, CA	35.7
	8							0614	0714	Summerland, CA	Sedgwick Reserve	69.7
IOP 10	1	2022				5	12	2231	2342	Sedgwick Reserve	Manzana Trailhead	40.8
	2						13	0156	0324	Manzana Trailhead	Sedgwick Reserve	36.9

## **Supplemental mobile and stationary data**

*Other data collected outside of the IOP and EOP structure of SWEX will be released later as separate datasets.*

## References

- Butterworth, B., et al., 2021: Connecting land-atmosphere interactions to surface heterogeneity in CHEESEHEAD19. *Bull. Amer. Meteor. Soc.*, **102**, E421-E445, <https://doi.org/10.1175/BAMS-D-19-0346.1>
- Straka, J.M., E.N. Rasmussen, and S.E. Fredrickson, 1996: A mobile mesonet for finescale meteorological observations. *J. Atmos. Ocean. Technol.*, **13**, 921–936.
- Waugh, S.M., 2012: The “U-Tube”: An Improved Aspirated Temperature System for Mobile Meteorological Observations, Especially in SevereWeather. Master’s Thesis, University of Oklahoma, Norman, OK, USA. Available online: <https://shareok.org/handle/11244/24679>.
- White, L., 2014: Mobile observations of a quasi-frontal transient moisture boundary in the Deep South. *Weather and Forecasting*, **29**, 1356-1373, DOI: <http://dx.doi.org/10.1175/WAF-D-14-00009.1>
- White, L., and M. Koziara, 2018: Surface thermodynamic gradients associated with Gulf of Mexico sea breeze fronts. *Adv. in Meteorol.*, 2018, 2601346, <https://doi.org/10.1155/2018/2601346>.
- White, L., 2020: Use of mobile measurements to investigate frontal structures in Mississippi. *J. Miss. Acad. of Sci.*, **65**, 170-182.
- White, L., and D. Lu, 2020: Multi-scale transects of three North American drylines. *Atmosphere*, **11**, 854, doi:10.3390/atmos11080854.
- White, Loren, 2021: Approaches to mesoscale pressure patterns from mobile data platforms. *Environ. Sci. Proc.*, **8**, 46, <https://doi.org/10.3390/ecas2021-10689>.